Analytical Treatments of Micro-channel and Micro-capillary Flows

Takahiro ADACHI [1],*, Rajamani Sambasivam [2], Franz DURST [3], David Filimonov[3]

* Corresponding author: Tel.: ++81 (18)889 2306; Fax: ++81 (18)889 2306 Email: adachi@ipc.akita-u.ac.jp
1: Department of Mechanical Engineering, Akita University, Japan
2: TATA Steel Limited Inc., India
3: FMP Technology GmbH, Germany

Abstract Extensive work in the field of micro-channel and micro-capillary flows using the extended Navier-Stokes equations are carried out in this paper by taking the diffusive mass transport into account and provided the basis for analytical treatments of these flows. The results are compared with experimental results for micro-channels and showed good agreement. It is found that a characteristic pressure is useful to explain the comparisons. In addition, the work on micro-channel flows is extended to micro-capillary flows, to provide analytical treatments of this class of flows. The analytical results show similar behavior to that of micro-channel flows. Comparisons between the analytical results and experimental findings are also presented and discussed by introducing the characteristic pressure.

Keywords: Extended Navier-Stokes equations, Diffusive mass flow, Characteristic pressure

1. Introduction

It is widely reported that in gaseous flows through micro-channel and micro-capillary, the measured mass flow rates can be higher than those obtained from the classical theory by solving the Navier-Stokes equations with no-slip boundary conditions at the wall for some given inlet and outlet pressure conditions. This increase of mass flow rate is one of the many strange phenomena which puzzles fluid flow researchers (Arkilic *et al*. (1997), Colin *et al*. (2004), Maurer *et al*. (2003) and Yang and Garimella (2009)). In order to bridge the gap between the experimental results and the theoretical predictions, micro-channel and micro-capillary flows are treated by introducing the assumptions that Maxwell slip velocities occur at the channel and capillary walls. Namely, the first or second order Maxwellian slip velocity models have been used at the wall as boundary conditions. A good summary of the work exists in the book of Karniadakis et al. (2005).

The assumptions of the Maxwell type of slip velocities at the walls of micro-channel and micro-capillary flows, however, are questioned in this study and it is argued that the difference between experimentally and theoretically obtained results of flow rates occurred due to

imperfections of the Navier-Stokes equations. Therefore, the modified equations called the extended Navier-Stokes ones are used in this study, where the extended Navier-Stokes equations should be written in terms of total velocity, refer Sambasivam and Durst (2010), made up of the convective velocity and the diffusive velocity terms. In addition, a different type of slip boundary conditions which is not the Maxwellian slip one but derived analytically from the physical insight is used for the diffusive velocity at the wall.

In this study, we have derived Stokes equations from the extended Navier-Stokes ones by applying the boundary-layer approximation for micro-channel and micro capillary, and obtained the analytical solutions for the velocities. By using the analytical solutions, we try to explain the difference between the experimental results and the theoretical predictions both for micro-channel and micro-capillary flows.

2. Mathematical treatment

2.1 Basic Equations

In this research of micro-channel and micro-capillary flows, we use the set of extended Navier-Stokes equations, which are written for the total velocity as suggested by Sambasivam

and Durst (2010). Assuming the flow to be two-dimensional in a rectangular co-ordinate system and axis symmetric in a cylindrical co-ordinate system, with no fluid flows in the tangential direction in the cylindrical co-ordinate, we obtain the equations as given bellow. Using the simple notations of (U, V) in the (x, r)-directions as the total velocities (see Figure 1), the set of extended, but two-dimensional Navier-Stokes equations can be written as follows:

$$\frac{\partial \rho}{\partial t} + \frac{\partial(\rho U)}{\partial x} + \frac{1}{r}\frac{\partial(r\rho V)}{\partial r} = 0 \tag{1}$$

$$\frac{\partial(\rho U)}{\partial t} + \frac{\partial(\rho U U)}{\partial x} + \frac{1}{r}\frac{\partial(r\rho U V)}{\partial r} =$$
$$-\frac{\partial P}{\partial x} + \frac{\mu}{3}\left\{\frac{\partial^2 U}{\partial x^2} + \frac{1}{r}\frac{\partial^2(rV)}{\partial x\partial r}\right\}$$
$$+ \mu\left[\frac{\partial^2 U}{\partial x^2} + \frac{\partial}{\partial r}\left\{\frac{1}{r}\frac{\partial(rU)}{\partial r}\right\}\right] \tag{2}$$

$$\frac{\partial(\rho V)}{\partial t} + \frac{\partial(\rho U V)}{\partial x} + \frac{1}{r}\frac{\partial(r\rho V V)}{\partial r} =$$
$$-\frac{\partial P}{\partial r} + \frac{\mu}{3}\left[\frac{\partial^2 U}{\partial x\partial r} + \frac{\partial}{\partial r}\left\{\frac{1}{r}\frac{\partial(rV)}{\partial r}\right\}\right]$$
$$+ \mu\left[\frac{\partial^2 V}{\partial x^2} + \frac{\partial}{\partial r}\left\{\frac{1}{r}\frac{\partial(rV)}{\partial r}\right\}\right] \tag{3}$$

where the viscosity μ is a constant, because only ideal gaseous flows are considered in this study, and the fluid flow is assumed to be isothermal. It should be noted that for the case of rectangular co-ordinates holds: $r = 1$ and $\partial / \partial r = \partial / \partial y$.

2.2 Order estimates

In order to derive the reduced form of the extended Navier-Stokes equations, we will apply order estimates as commonly used in boundary layer theory. These take into account that the length scale of the flow in the streamwise direction is much larger than that perpendicular to the wall. First, we can assume for all micro-conduit flows, considered in this paper that the flow field is steady and fully developed, and the non-linear terms are negligible because they are very small in micro-channel and micro-capillary flows.
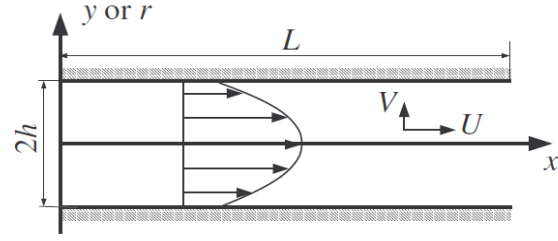

Fig.1 Sketch of velocity profiles for the extended Navier-Stokes equations.

Introducing these assumptions, Eqs. (1)-(3) can be rewritten as follows:

$$\frac{\partial(\rho U)}{\partial x} + \frac{1}{r}\frac{\partial(r\rho V)}{\partial r} = 0 \tag{4}$$

$$0 = -\frac{\partial P}{\partial x} + \frac{\mu}{3}\left\{\frac{\partial^2 U}{\partial x^2} + \frac{1}{r}\frac{\partial^2(rV)}{\partial x\partial r}\right\}$$
$$+ \mu\left[\frac{\partial^2 U}{\partial x^2} + \frac{\partial}{\partial r}\left\{\frac{1}{r}\frac{\partial(rU)}{\partial r}\right\}\right] \tag{5}$$

$$0 = -\frac{\partial P}{\partial r} + \frac{\mu}{3}\left[\frac{\partial^2 U}{\partial x\partial r} + \frac{\partial}{\partial r}\left\{\frac{1}{r}\frac{\partial(rV)}{\partial r}\right\}\right]$$
$$+ \mu\left[\frac{\partial^2 V}{\partial x^2} + \frac{\partial}{\partial r}\left\{\frac{1}{r}\frac{\partial(rV)}{\partial r}\right\}\right] \tag{6}$$

As representative length scale quantities, to perform order estimates, we can adopt L as a length scale in the streamwise direction and h as a length scale in direction perpendicular to the wall, where $h \ll L$. With U being the representative velocity in the streamwise direction, the velocity component V normal to the wall must be small. This can be deduced from the continuity Eq. (4), yielding:

$$V \sim O\left(\frac{Uh}{L}\right) \ll U \tag{7}$$

because $h \ll L$, as stated above for micro-conduit flows.

Next, we can perform order estimates for the viscous terms in Eq. (5) to yield:

$$\mu\frac{\partial}{\partial r}\left\{\frac{1}{r}\frac{\partial(rU)}{\partial r}\right\} \sim O\left(\frac{\mu U}{h^2}\right), \tag{8}$$

$$\mu\frac{\partial^2 U}{\partial x^2} \sim O\left(\frac{\mu U}{L^2}\right), \quad \frac{\mu}{r}\frac{\partial^2(rV)}{\partial x\partial r} \sim O\left(\frac{\mu U}{L^2}\right) \tag{9}$$

We can see that the order of magnitude of the term in Eq. (8) is much larger than all the other terms of Eq. (9). Therefore, we must accept the fact, without further arguments, that the

term of Eq. (8) cannot be neglected. For this reason, the order of the pressure gradient term in Eq. (5) must be comparable with the term of Eq. (8) and can be estimated to be:

$$\frac{\partial P}{\partial x} \sim O\left(\frac{P}{L}\right) \tag{10}$$

Estimating the order of magnitude of Eq. (10) with respect to the term in Eq. (8), the order of magnitude of the pressure is obtained as:

$$P \sim O\left(\frac{\mu U L}{h^2}\right) \tag{11}$$

On the other hand, we can estimate the order of the pressure gradient term in Eq. (6) as:

$$\frac{\partial P}{\partial r} \sim O\left(\frac{\mu U L}{h^3}\right) \tag{12}$$

As for the viscous terms in Eq. (6), we can estimate the order of magnitude of the following terms as:

$$\mu \frac{\partial^2 V}{\partial x^2} \sim O\left(\frac{\mu U h}{L^3}\right) \tag{13}$$

$$\mu \frac{\partial^2 U}{\partial x \partial r} \sim \mu \frac{\partial}{\partial r}\left\{\frac{1}{r}\frac{\partial(rV)}{\partial r}\right\} \sim O\left(\frac{\mu U}{hL}\right) \tag{14}$$

The order of the terms (13) and (14) are smaller than the pressure gradient term of Eq. (12). Therefore, we can neglect the viscous terms in equation (6) compared with the pressure gradient term obtaining:

$$\frac{\partial P}{\partial r} = 0 \tag{15}$$

It should be noted that the pressure depends only on the *x*-direction so that $P = P(x)$ and it means that the density also depends only on *x*-direction as $\rho = \rho(x)$. Finally we obtain the following approximated equation for micro-channel and micro-capillary flows:

$$0 = -\frac{dP}{dx} + \mu\frac{1}{r}\frac{d}{dr}\left(r\frac{dU}{dr}\right) \tag{16}$$

where $r = 1$ and $d/dr = d/dy$ yields the equation for micro-channel flows.

3. Theoretical solutions for each case

3.1 Micro-channel flows

To obtain an analytical solution for fully developed micro-channel flows, we will solve Eq. (16), expressed in rectangular co-ordinates, with the boundary condition (Sambasivam and Durst (2010)) at the wall as

$$\rho U = -\frac{\mu}{P}\frac{dP}{dx} \quad \text{at} \quad y = \pm h \tag{17}$$

Then the analytical solution in a micro-channel can be written as:

$$\rho U = -\frac{\rho}{2\mu}(h^2 - y^2)\frac{dP}{dx} - \frac{\mu}{P}\frac{dP}{dx} \tag{18}$$

It should be noted that the second term of the right hand side terms arises from the diffusion influence, and the diffusive part of the mass flow rate will only make strong contributions to the velocity for low pressures P.

From Eq. (18) we can derive the relation between the total mass flow rate M^T, the diffusive mass flow rate M^D and the pressure. Therefore, by integrating Eq. (18), first in the cross flow and second in the flow directions, we can derive the relation for the total mass flow rate:

$$\begin{aligned}
M^T &= w\int_{-h}^{h}(\rho U)dy \\
&= -w\int_{-h}^{h}\left\{\frac{\rho}{2\mu}(h^2 - y^2)\frac{dP}{dx} + \frac{\mu}{P}\frac{dP}{dx}\right\}dy \\
&= -2hw\left(\frac{h^2 P}{3\mu RT} + \frac{\mu}{P}\right)\frac{dP}{dx}
\end{aligned} \tag{19}$$

where w is a width of the micro-channel. Integrating Eq. (19) from the inlet ($x = 0$) to the outlet ($x = L$), we can obtain:

$$M^T = \frac{h^3 w P_{out}^2}{3\mu LRT}\left\{\left(\frac{P_{in}}{P_{out}}\right)^2 - 1\right\} + \frac{2\mu hw}{L}\ln\left(\frac{P_{in}}{P_{out}}\right) \tag{20}$$

Therefore, the total mass flow rate M^T can be expressed as a function of the pressure ratio P_{in}/P_{out}. Furthermore, we will proceed to obtain an universal relationship between the total mass flow rate and pressure. Therefore, Eq. (19) can be rewritten as

$$M^T = -2hw\frac{\mu}{P}\frac{dP}{dx}\left(\frac{h^2 P^2}{3\mu^2 RT} + 1\right) \tag{21}$$

Since the pressure P is constant in the *y*-direction, the diffusive mass flow rate M^D can be expressed by integrating Eq. (17) over a

cross sectional area to obtain:

$$M^D = -2hw\frac{\mu}{P}\frac{dP}{dx} \tag{22}$$

Substituting Eq. (22) into Eq. (21) yields:

$$\frac{M^D}{M^T} = \frac{1}{\frac{h^2 P^2}{3\mu^2 RT} + 1} \tag{23}$$

Defining the characteristic pressure as $Pc = \mu\sqrt{3RT}/h$, we can rewrite Eq. (23) as follows:

$$\frac{M^D}{M^T} = \frac{1}{(\frac{P}{P_c})^2 + 1} \tag{24}$$

The above final equation is an universal relation between the local mass flow rate and the normalized local pressure.

3.2 Results for micro-channel

Using the above equations, we can calculate the total mass flow rates of a Helium gas flow in a micro-channel with the same conditions corresponding to the experiments of Maurer *et al.* (2003) whose conditions are summarized in Tab.1. The total mass flow rates M^T for the outlet pressure P_{out} changing from 0.012 to 0.1 MPa are shown in Fig. 2 together with experimental results of Maurer *et al.* (2003), where the axis of abscissas is taken as $0.5(P^2_{in} - P^2_{out})$ according to the notation of Maurer *et al.* (2003).

Figure 2 shows that the choice of the outlet pressure conditions is relevant to obtain the typical micro-channel effects on the gas flow. It can be seen that, as the outlet pressure is decreased, the deviation of the total mass flow rate, obtained from the extended Navier-Stokes equations, increases with respect to the convective mass flow rate obtained from the compressible Navier-Stokes equations with no-slip boundary conditions. The total mass flow rate especially for P_{out} = 0.012 MPa shows considerable deviation from predictions based on the Navier-Stokes equations with no-slip conditions. The present analytical result of P_{out} = 0.012 MPa yields good agreement with experimental results of Maurer *et al.* (2003) and the analytical deduced solution follows the micro-channel effect that occurred in the experiment. This finding is a good proof that
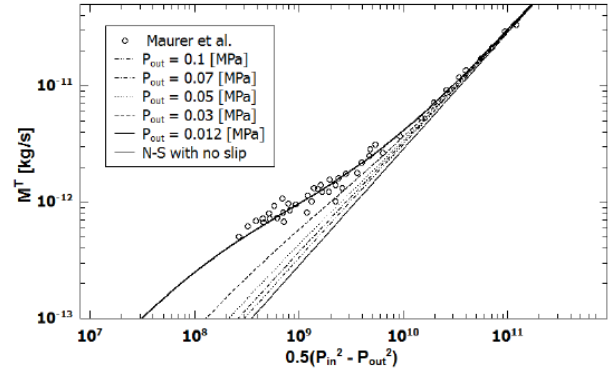

Fig.2 Total mass flow rate vs. the difference of squares of pressure of P_{in} and P_{out}

Table 1 Experimental conditions of [1] Maurer *et al.* (2003) and [2] Arkilic *et al.* (1997).

Experimental Parameters	[1]	[2]
Gas used	Helium	Helium
Temperature [K]	293	314
Outlet pressure P_{out} [MPa]	$0.012 \sim 0.1$	0.1
Dynamic viscosity [10^{-5} Pa · s]	1.99	2.066
Gas constant [J/kg·K]	2077	2077
Height h [μm]	0.57	0.665
Width w [μm]	200	52.25
Length L [μm]	10000	7500
Characteristic pressure P_c [MPa]	0.0477	0.0435

the order estimate, carried out in this study, yields the equation which describes physically well the flow in micro-channels.

Using the derived analytical solutions, we can understand why the deviation between the mass flow rates obtained from the extended Navier-Stokes equations and the classical theory is decreased as $(P^2_{in} - P^2_{out})$ is increased. This means that the increase of the pressure ratio P_{in}/P_{out} reduces the deviation between the mass flow rates. This behavior can be explained by equation (20). Namely, a significant deviation from the classical theory appears at lower pressure ratios for a given outlet pressure P_{out}, because the diffusion effect is proportional to the term of $\ln(P_{in}/P_{out})$ and the order of $\ln(P_{in}/P_{out})$ is comparable with one of $(P_{in}/P_{out})^2$ only for the smaller pressure ratio. This implies that the diffusion is effective for the micro-channel flow only when the pressure range P is absolutely small and the pressure ratio (P_{in}/P_{out}) between the

inlet and outlet is also small. In addition, we calculate the mass flow rates for the different pressure conditions, corresponding to Arkilic *et al.* (1997) and Colin *et al.* (2004) whose conditions are summarized in Table 1 and 2. These comparisons of the analytical results with the experimental ones are shown in Figs. 3 and 4, where the horizontal axes are taken as the pressure ratio. In the figures, the results obtained from the extended Navier-Stokes equations are shown by solid lines, while the ones by the classical compressible Navier-Stokes equations with no-slip boundary conditions are shown by dashed lines. We can see that the diffusion effects are presented but they are quite small. This is mainly because the pressures in the experiments of Arkilic *et al.* (1997) and Colin *et al.* (2004) are larger and we, therefore, do not get the micro-channel effect.

In order to explain why the diffusion effect is small, the relation between the mass flow rate and the characteristic pressure defined by equation (24) is shown in Fig. 5. We can see, that the diffusive mass flow rate reaches 50 % of the total mass flow rate for the case of $P/P_c = 1$. This means that the convective and the diffusive mass flow rates are of the same order in the total mass flow rate. The characteristic pressure ratio of P/P_c ranges as $P_{in}/P_c > P/P_c > P_{out}/P_c$. With the decrease of the pressure from P_{in} to P_{out}, the diffusive effect starts to grow in importance, since the characteristic pressure ratio P/P_c is decreased. If the inlet and outlet pressures are chosen to lie close to the characteristic pressure, the total mass flow rate increases due to the strong effect of the self-diffusion and this yield the considerable deviation from the predictions based on the classical Navier-Stokes equations.

In Fig. 5, the pressure ranges of the experimental data of (I) - Maurer *et al.* (2003), (II) - Arkilic *et al.* (1997) and (III) Colin *et al.* (2004) are presented. As previously mentioned, the strong diffusion effect was analytically obtained for the experimental conditions of Maurer et al.(2003). Their strong micro-channel effects can be explained now with the help of the characteristic pressure, since the pressure ratios are quite small and the pressure

range is close to the characteristic pressure P_c of the experimental setup. On the other hand, in the experimental conditions of Arkilic et al. (1997) and Colin et al. (2004), the chosen pressures in the experiments are larger compared with their characteristic pressures. Therefore, only small diffusion effects are present. Knowing that the diffusive effect is significant for low pressures (or for high temperatures), the outlet pressure at the exit of the micro-channel should be taken very small to experimentally show the typical micro-channel effect at room temperatures.
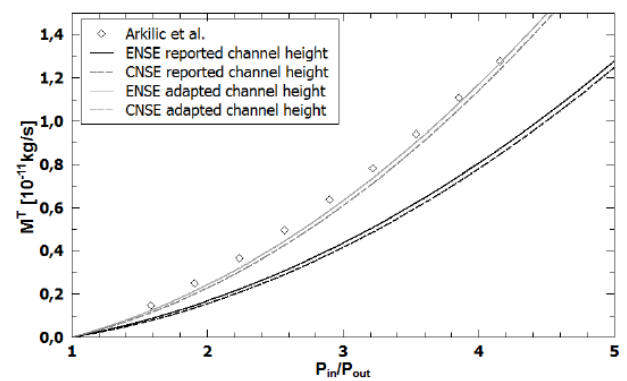

Fig.3: Total mass flow rate vs. pressure ratio for experiments of Arkilic et al. (1997)

Table 2: Experimental conditions of Colin *et al.* (2004).

Experimental Parameters	Case a	Case b	Case c	Case d
Gas used	Nitrogen	Nitrogen	Helium	Helium
Temperature [K]	294.2	294.2	294.2	294.2
Outlet pressure [10^5 Pa]	2	0.65	1.9	1.026
Dynamic viscosity [10^{-6} Pa·s]	19.0	19.0	17.5	17.5
Gas constant [J/kg·K]	296.9	296.9	2077	2077
Channel length [μm]	5000	5000	5000	5000
Channel width [μm]	21.2	21.2	21.2	21.2
Reported channel height [μm]	1.88	1.88	1.88	1.88
Adapted channel height [μm]	1.94	2.06	1.94	2.06

Although the choice of the pressure range for the experiments has been shown to be the reason why the diffusion effect is small under the conditions of Arkilic *et al.* (1997) and Colin *et al.* (2004), a considerable discrepancy between the present analytical predictions and the corresponding experimental results still exists.

The discrepancy can be attributed either to incorrect pressure distributions or to the measurement errors of the flow rate in the mentioned experiments. As shown previously,
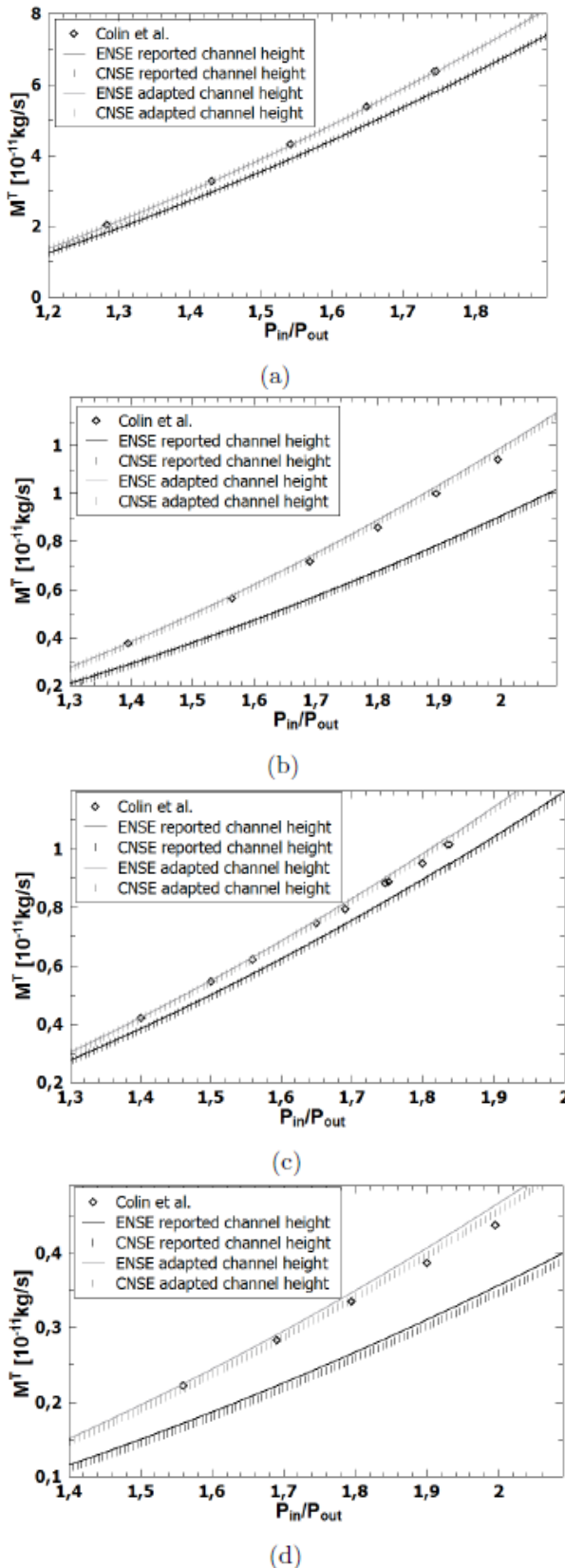
(a)

(b)

(c)

(d)

Fig.4: Total mass flow rate vs. pressure ratio for experiments of Colin et al. (2004)
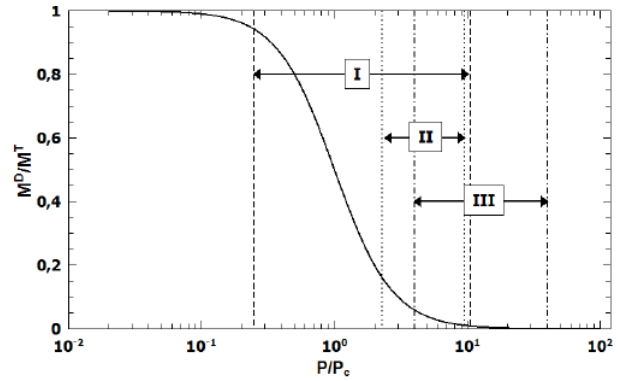

Fig.5: Fraction of mass flow rate vs. pressure.

the experiments conducted by Arkilic *et al.* (1997) and Colin *et al.* (2004) lay in the convection-dominated region, i.e. in the pressure region where the diffusion effect is small. Therefore, the main reason for the discrepancy may be measurement errors during their experiments. Colin *et al.* (2004) reported an uncertainty of about 10% for the measurement of the channel height. Such an uncertainty of the measurement of the channel height can cause the discrepancy between the experimental data and theoretical predictions.

In order to examine the possibility of the uncertainty effect on the discrepancy between the present analytical solution and the corresponding experimental results, we attempted to calculate the mass flow rate for the slightly different conditions of the experiments of Arkilic *et al.* (1997) and Colin *et al.* (2004). Using a 10% greater channel height to calculate the total mass flow rates in case of Arkilic *et al.* (1997) and a 3 - 10% greater channel height in the four cases of Colin *et al.* (2004) (see Table 2), one can obtain very good agreement between the present analytical results and the mentioned experimental data, as shown in Figures 3 and 4. The adapted channel height for each case of Colin *et al.* (2004) is also reported in Table 2.

Concluding this section, we point out that the measurement accuracy can be seen as one of the prime factors of the discrepancy between the present analytical results and the experimental data. It should be noted that there was no difference in the experimental conditions of Arkilic *et al.* (1997) and Colin *et al.* (2004) between the mass flow rates obtained by the extended Navier-Stokes

equations (ENSE) and the classical Navier-Stokes equations (CNSE) with no-slip conditions, because the pressures chosen in their experiments were in the convection-dominated range.

3.3 Micro-capillary flows

To obtain an analytical solution for fully developed micro-capillary flows, we will solve Eq. (16) of the cylindrical co-ordinates in a similar way. Then the analytical solution for the total velocity in micro-capillary flows can be written as:

$$\rho U^T = -\frac{\rho}{4\mu}(h^2 - r^2)\frac{dP}{dx} - \frac{\mu}{P}\frac{dP}{dx} \quad (25)$$

In addition, we can obtain the relations between the total mass flow rate M^T, its diffusive part M^D and the pressure as

$$M^T = \frac{\pi h^4 P_{out}^2}{16\mu LRT}\left\{\left(\frac{P_{in}}{P_{out}}\right)^2 - 1\right\} + \frac{\mu\pi h^2}{L}\ln\left(\frac{P_{in}}{P_{out}}\right)$$

$$(26)$$

$$\frac{M^D}{M^T} = \frac{1}{(\frac{P}{P_c})^2 + 1} \quad (27)$$

where a characteristic pressure P_c is $P_c = \mu\sqrt{8RT}/h$. The above final equation (27) describes an universal relation between the local mass flow rate and the local normalized pressure in micro-capillary flows.

3.4 Results for micro-capillary

In this section, we want to prove our analytical solution for micro-capillary flows by comparison of the results with corresponding experimental data, available in the literature. In this context, Figure 6 shows the total mass flow rates obtained by Yang and Garimella (2009) as a function of pressure ratio P_{in}/P_{out}. The experimental conditions of Yang and Garimella (2009) are reported in Table 3. The present results obtained from the extended Navier-Stokes equations (solid lines) and ones obtained from the classical compressible Navier-Stokes equations (dashed lines) with no-slip boundary conditions are also shown in Fig. 6. The analytical results
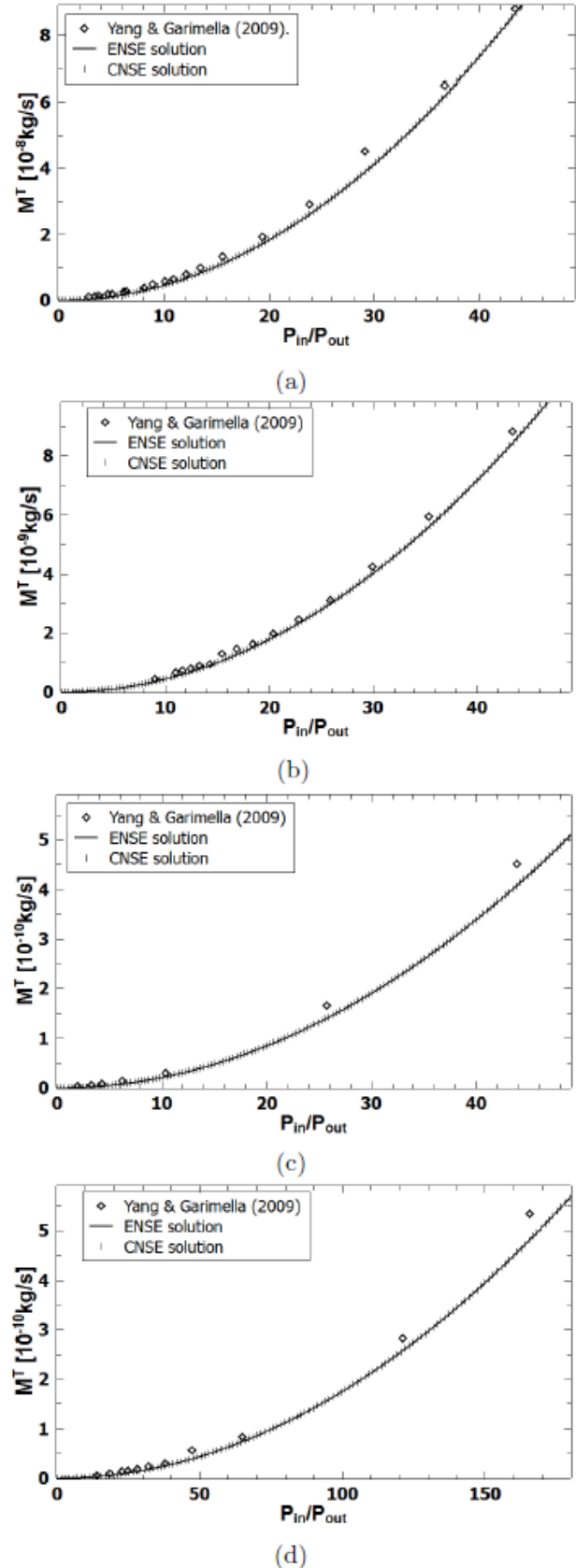

(a)

(b)

(c)

(d)

Fig.6: Total mass flow rate vs. pressure ratio for experiments of Yang and Garimella (2009)

Table 3: Experimental conditions of Yang and Garimella (2009).

Experimental Parameters	Case a	Case b	Case c	Case d
Gas used	Air	Air	Air	Air
Temperature (K)	293	293	293	293
Outlet pressure P_{out} (Pa)	2337	2337	2337	608
Dynamic viscosity (10^{-5} Pa · s)	1.82	1.82	1.82	1.82
Gas constant (J/kg·K)	287	287	287	287
Radius h (μm)	50	25	10	10
Length L (μm)	95000	61000	33000	27000
Characteristic pressure P_c (Pa)	298.6	597.2	1493	1493

Fig.7: fraction of the mass flow rate vs. pressure ratio

show no difference between the solution of the classical and the extended Navier-Stokes equation for all considered cases of Yang and Garimella (2009) and also a good agreement with the experimental data.

As already explained for micro-channel flows, we can only obtain typical micro-capillary effects when the inlet and outlet pressures are both chosen to lie close to the characteristic pressure of the experimental setup so that the fraction of the diffusive mass flow rate on the total mass flow rate is significant. In this context, Fig. 7 shows the ratio of M^D/M^T as a function of the characteristic pressure ratio P/P_c together with the experimental pressure ranges of Yang and Garimella (2009). In cases (a) and (b) almost no influence of the diffusive mass flow rate on the total mass flow rate is expected, since both inlet and outlet pressure are chosen much higher than the characteristic pressure of considered experiments. In cases (c) and (d) the outlet pressure is chosen to lie close to the characteristic pressure P_c, so that the diffusive mass flow rate dominates the flow at least in the part of the micro-capillary which is closer to the outlet. With increase of the pressure ratio for a constant outlet pressure, i.e. increase of the inlet pressure, the influence of the diffusive mass flux on the total mass flow rate reduces. This can be explained with equation (26). The term containing $\ln(P_{in}/P_{out})$ in this equation describes the diffusive part of the total mass flow rate and the other term containing $(P_{in}/P_{out})^2$ of its convective part. For higher pressure ratio the diffusive part of the total mass flow rate becomes negligible and the difference between the extended and classical solution of the Navier-Stokes equation disappears.
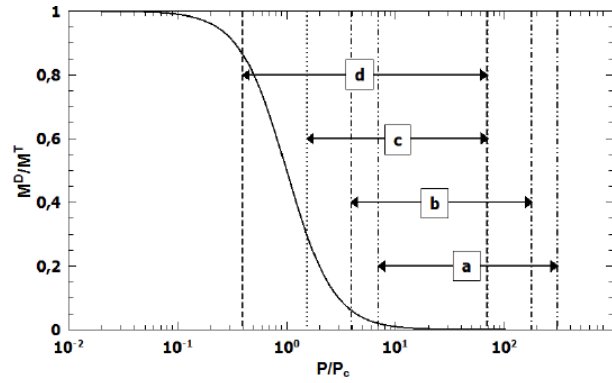
5. Summary

Using the extended Navier-Stokes equations, we can explain the physics behind the typical "micro-channel effects". It is shown that for certain experimental conditions the diffusive effects in the micro-conduit flows become significant and the total mass flow rate shows considerable deviations from the classical theory.

A characteristic pressure for micro-channel and micro-capillary flows is introduced in this work. At such a characteristic pressure the flow in micro-conduit starts to behave differently. Namely, for pressure values less than the characteristic pressure the flow is dominated by diffusion. In case that the local pressure is higher than the characteristic one, the flow is dominated by convection. As already mentioned the diffusive mass flow causes the difference between the classical and the extended Navier-Stokes equations and is also the reason for the deviations of the experimental results from predictions of the classical theory. To show the typical "micro-conduit effect" in experiment the inlet and outlet pressure should be chosen to lie close to the characteristic pressure of the experimental setup.

References

Arkilic, E. B., Schmidt M. A., Member of IEEE & Breuer, K. S. 1997 Gaseous slip Flow in long microchannels. J. MEMS **6**,167-178.
Colin, S., Lalonde, P. & Caen, R. 2004

Validation of a second-order slip flow model in rectangular microchannels. Heat Transfer Engineering **25** 23-31.

Maurer, J., Tabeling, P., Joseph, P. & Willaime, H. 2003 Second-order slip laws in Microchannels for helium and nitrogen. Phys. Fluids **15**, 2613-2621.

Karniadakis, G., Beskok, A. & Aluru, N. 2005 Microflows and nanoflows: Fundamentals and simulation. Springer.

fluid mechanics equations and their Applications to unsolved flow problems, submitted to Phys. Fluids.

Yang, Z. & Garimella, S. V. 2009 Rarefied gas flow in microtubes at different inlet-outlet pressure ratios. Physics of Fluids **21** 052005. 35

Sambasivam, R. & Durst, F. 2010 Extended